



# Timothy Grass Pollen Induces Spatial Reorganisation of F-Actin and Loss of Junctional Integrity in Respiratory Cells

Peta Bradbury<sup>1</sup>, Aylin Cidem<sup>1</sup>, Hadi Mahmodi<sup>3</sup>, Janet M. Davies<sup>4</sup>, Patrick T. Spicer<sup>5</sup>, Stuart W. Prescott<sup>5</sup>, Irina Kabakova<sup>3</sup>, Hui Xin Ong<sup>1,2,6</sup> and Daniela Traini<sup>1,2,6</sup> 

Received 22 August 2021; accepted 13 December 2021

**Abstract**— Grass pollens have been identified as mediators of respiratory distress, capable of exacerbating respiratory diseases including epidemic thunderstorm asthma (ETSA). It is hypothesised that during thunderstorms, grass pollen grains swell to absorb atmospheric water, rupture, and release internal protein content to the atmosphere. The inhalation of atmospheric grass pollen proteins results in deadly ETSA events. We sought to identify the underlying cellular mechanisms that may contribute towards the severity of ETSA in temperate climates using Timothy grass (*Phleum pratense*). Respiratory cells exposed to Timothy grass pollen protein extract (PPE) caused cells to undergo hypoxia ultimately triggering the subcellular re-organisation of F-actin from the peri junctional belt to cytoplasmic fibre assembly traversing the cell body. This change in actin configuration coincided with the spatial reorganisation of microtubules and importantly, decreased cell compressibility specifically at the cell centre. Further to this, we find that the pollen-induced reorganisation of the actin cytoskeleton prompting secretion of the pro-inflammatory cytokine, interleukin-8. In addition, the loss of peri-junctional actin following exposure to pollen proteins was accompanied by the release of epithelial transmembrane protein, E-cadherin from cell–cell junctions resulting in a decrease in epithelial barrier integrity. We demonstrate that Timothy grass pollen regulates F-actin dynamics and E-cadherin localisation in respiratory cells to mediate cell–cell junctional integrity highlighting a possible molecular pathway underpinning ETSA events.

**KEY WORDS:** Actin dynamics; E-cadherin; Hypoxia; Membrane integrity; Brillouin microscopy; Thunderstorm asthma; Timothy grass pollen.

## INTRODUCTION

Epidemic thunderstorm asthma (ETSA) is a term used to describe the phenomenon of increased acute bronchospasms triggered by the occurrence of thunderstorms in a local vicinity [1, 2]. While the causation of ETSA events is not fully understood, it is known that the

<sup>1</sup>Respiratory Technology, Woolcock Institute of Medical Research, Sydney, Australia

<sup>2</sup>Macquarie Medical School, Faculty of Medicine, Health and Human Sciences, Macquarie University, Sydney, Australia

<sup>3</sup>School of Mathematical and Physical Sciences, University of Technology Sydney, Sydney, Australia

<sup>4</sup>School of Biomedical Science, Centre for Immunology and Infection Control, Queensland University of Technology, Brisbane, Australia

<sup>5</sup>School of Chemical Engineering, UNSW, Sydney, Australia

<sup>6</sup>To whom correspondence should be addressed at and Respiratory Technology, Woolcock Institute of Medical Research, Sydney, Australia. Email: [huixin.ong@mq.edu.au](mailto:huixin.ong@mq.edu.au) [daniela.traini@mq.edu.au](mailto:daniela.traini@mq.edu.au)

combination and concentrations of allergen particles in circulation, the sudden change in meteorological conditions and individual susceptibility, are necessary for facilitating the ETSA phenomenon [3]. ETSA events are generally characterised by an abundance of aeroallergens, most notably the high content of grass pollen grain proteins [1]. Importantly, not all thunderstorms are accompanied by ETSA events, suggesting that the species of pollen grain(s) present within a local area may be a factor that influences ETSA severity [4].

Direct respiratory exposure and inhalation of highly concentrated, pollen-based aeroallergens during thunderstorms is known to increase the risk of ETSA events in specific climates. The largest recorded ETSA event globally occurred in Melbourne (Victoria, Australia) in 2016, where the pollen count was classified as 'Extreme' ( $\geq 100$  grains/m<sup>3</sup>) with temperate grass pollens, Ryegrass (*Lolium perenne*), and Timothy grass (*Phleum pratense*) comprising the majority of the total pollen content [5, 6]. This extreme, local, high concentration of pollen resulted in an unprecedented number of people suffering acute respiratory distress and culminated in 9 deaths [5, 6]. Yet, the cellular mechanisms that underpin respiratory exacerbations like the Melbourne 2016 ETSA event are unknown and the role individual pollen species play in mediating respiratory changes at the cellular level remains unclear.

Actin is an essential cytoskeletal protein important in maintaining and regulating many biological processes including cell shape, ion transport, and receptor-mediated signalling in response to extracellular stimuli [7]. Importantly, exposure to extracellular stimulus can induce and dictate modifications to filamentous-actin (F-actin) causing spatial and temporal reorganisations that influence changes in cell shape, size, and function and initiate pathophysiological phenotypes [8–11]. In respiratory cells, actin plays a key role in regulating both ion and solute transport, and also integrity of the epithelial barrier via interactions with specific cell-cell junctional proteins [12–14]. The adherent protein, E-cadherin, localises at the cellular boundaries of cell–cell junctions to stabilise and maintain functional integrity of the junctional barrier [15]. As such, E-cadherin dysfunction either via mutation or aberrant localisation to cell–cell junctions has been associated with pathophysiological changes to respiratory cellular barrier function, integrity, and the progression of disease states [16]. Thus, both actin and E-cadherin play a vital role in preserving respiratory junctional barrier integrity and respiratory homeostasis, yet little is known of their role in pollen mediated asthma events, including

ETSA. The present study sought to identify the molecular response of respiratory cells following exposure to temperate grass pollen protein extracts of Timothy grass. Specifically, we investigate the subcellular organisation and localisation of both actin and E-cadherin following exposure to Timothy grass pollen proteins.

## METHODS

### Scanning Electron Microscopy

The surface morphology of whole Ryegrass and Timothy grass pollens was evaluated using JEOL JCM-6000 scanning electron microscopy (SEM; JOEL, USA). Samples were dispersed onto carbon sticker tabs and gold sputter-coated for 2 min (Smart Coater, JOEL) to a thickness of approximately 20 nm. Images were captured at 5 kV at 500 $\times$  and 1000 $\times$  magnifications.

### Preparation of Grass Pollen Protein Extracts

Non-defatted Ryegrass and Timothy grass pollen (Greer Laboratories, USA) proteins were extracted as described previously [17]. Ryegrass and Timothy grass PPEs (10  $\mu$ g) were visualised on a 10% polyacrylamide gel following SDS-PAGE and stained with Coomassie Brilliant Blue R-250 (Sigma-Aldrich). Colorimetric images were captured using the BioRad EZ Imager (BioRad, USA).

### Cell Line Maintenance

The A549 cell line was purchased from the American Type Cell Culture Collection (ATCC). Cells were maintained in Dulbecco's modified Eagle medium (DMEM):F12 (Sigma-Aldrich) supplemented with 10% (v/v) heat-inactivated foetal bovine serum (FBS; Invitrogen), 0.5 mM L-glutamine (Invitrogen, USA), and 1% (v/v) non-essential amino acids (Sigma-Aldrich) at 37 °C with 5% CO<sub>2</sub>. Cells were seeded at 3  $\times$  10<sup>4</sup> cells/cm<sup>2</sup>, used between passage numbers 98 and 136. Cells were quiesced for 24 h and then exposed to grass PPE (0.05, 0.5 and 5 mg/mL) for 24 h.

### Immunofluorescence and Image Analysis

Cells were fixed with 4% (v/v) paraformaldehyde, blocked, and permeabilised in 5% (v/v) normal goat serum

(Invitrogen, USA) and 0.3% (v/v) Triton X-100. Cells were incubated with anti-E-cadherin (HECD-1; 1:100) (Abcam; USA) and counterstained with DAPI (1:10,000) and TRITC-Phalloidin (1:2000). To visualise tubulin, cells were fixed with ice-cold methanol and blocked with 5% normal goat serum (v/v) (Invitrogen) and 0.3% Triton X-100 (v/v). Cells were incubated with  $\alpha$ -tubulin (DM1A; 1:1000) (Sigma-Aldrich) followed by secondary antibody incubation of Alexa Fluor 488 (Whole IgG; 1:1000) (Jackson Immuno Research Laboratories, USA).

### Protein Extraction and Immunoblotting

Cells were treated with grass PPE (0.05, 0.5, and 5 mg/mL) for 24 h prior to whole cell lysate collection. Cells were placed on ice and washed twice with PBS. Cells were scraped and extracted in 0.1% SDS-RIPA lysis buffer (50 mM Tris, 150 mM NaCl, 5 mM EDTA, 1% (v/v) Nonidet P-40, 0.1% (w/v) SDS, 1% (w/v) Na Deoxycholate). Lysates were centrifuged  $15,500 \times g$  for 10 min at 4 °C and supernatants collected. Whole-cell lysates (10  $\mu$ g) were subjected to gel electrophoresis and transferred onto methanol-activated Immobilon PVDF membrane. Membranes were probed with anti-E-cadherin (1:1000; HECD-1), anti-actin (1:5000; AC-40, Sigma-Aldrich), anti- $\alpha$ -tubulin (1:5000; DMA1A, Sigma), GAPDH (1:5000; Sigma-Aldrich), or HSP-70 (1:5000; Sigma-Aldrich) and visualised using the BioRad ChemiDoc (BioRad).

### Membrane Integrity

To determine the integrity of A549 cell lipid membranes, cells were pre-loaded with Calcein-AM and then exposed to PPE as previously described [18] A549 cells were incubated with 0.5  $\mu$ M Calcein-AM (Invitrogen) for 15 min at 37 °C, cells were washed with PBS, and Timothy grass PPE was added (supplemented with 20 mM HEPES). Cells were immediately imaged using the Nikon Ti Eclipse inverted microscope with an S Plan Fluor ELWD 20 $\times$ Ph1 ADM objective equipped with a CoolSnap ES2 camera for 90 min, with images taken every 5 min. Images were analysed using Fiji.

### Detection of Reactive Oxygen Species

Reactive oxygen species (ROS) produced by A549 cells following 24 h post exposure of PPE was measured

by incubating cells with 50  $\mu$ M 2', 7'-dichlorofluorescein diacetate (DCFDA; Sigma-Aldrich) for 15 min at 37 °C prior to reading the fluorescence (Ex/Em 488/530 nm) using the SpectraMax iD3 microplate reader. Positive control cells were treated with 200  $\mu$ M of Menadione K3 (Vitamin K3; Sigma-Aldrich), while negative controls were treated with 10 mM of N-Acetyl-L-Cysteine (NAC; Sigma-Aldrich).

### Enzyme-Linked Immunosorbent Assay

Interleukin-6 and -8 (IL-6, IL-8) production were determined using the enzyme-linked immunosorbent assay (ELISA) kits (BD OptEIA, BD Biosciences) according to manufacturer's guidelines. Supernatants were collected from A549 cells treated with grass pollen protein extract for 24 h. Untreated cells served as the control.

To determine the role of actin in proinflammatory cytokine production, quiesced cells were washed with PBS and permeabilised with 0.22 pmol/cell Triton-X-100 [19] and incubated with phalloidin for 10 min. Cells were then washed and allowed to recover overnight prior to exposure to grass pollen protein extract. Supernatants were collected 24 h post exposure, and IL-8 cytokine expression was measured.

### Microscopy and Image Analysis

All cells were imaged at identical settings using the Nikon Ti Eclipse inverted microscope with an S Plan Fluor ELWD 40X Ph2 ADM objective equipped with a CoolSnap ES2 camera. For fixed, immunofluorescent images of a minimum of 20 random fields of view were imaged. Images were analysed using open-source software CellProfiler (v3.1.9) [20] (<http://cellprofiler.org/>). Briefly, DAPI stained images were used to segment and identify the nucleus following a minimum cross entropy thresholding method, while cells were segmented using the Otsu intensity threshold method. Actin- and E-cadherin-stained images were subjected to identical thresholding methods and parameters (actin: Otsu; E-cadherin: Robust Background; Tubulin: Otsu). Individual cells were binned with 10 equidistant, scaled bins applied to each cell, and the mean fluorescence intensity was measured for per bin (Bin 1 = cell centre and Bin 10 = cell boundary).

## Electric Cell-Substrate Impedance Sensing

The integrity of A549 cell–cell junctions was assessed using the electric cell-substrate impedance sensing system (ECIS; Applied BioPhysics Inc., USA). ECIS 8W10E + arrays were coated with 10 mM L-cysteine prior to cell seeding. Real-time transepithelial electrical resistance (TEER) data were captured every 5 min for 24 h, and resistance was measured at 8000 Hz. The initial 5 h were excluded to allow apparatus equilibration.

## Brillouin Microscopy

Brillouin microscopy was utilised to assess viscoelastic and compressibility properties of PFA fixed cells immersed in PBS that had previously been treated with Timothy grass PPE for 24 h. A total of 35  $\mu\text{m} \times 35 \mu\text{m}$  maps of Brillouin frequency shift (BFS) were measured across cellular samples and then normalised to BFS measurements of cell-free regions. The Brillouin microscopy system comprised of a continuous wave 660-nm laser (Cobolt, Flamenco), a confocal microscope (CM1, JRS Instruments) and a scanning tandem Fabry–Perot interferometer (TFP1, JRS Instruments), using an immersion objective lens with 60 $\times$  magnification (Nikon, NA = 1, WD = 2.8 mm). Brillouin data was collected using in-house software to perform two-dimensional (2D) scans within plane spatial resolution of approximately 1  $\mu\text{m}$  and an acquisition time per point of 20 s. To prevent sample damage by incident radiation, the laser power was less than 20 mW. The raw spectra of Brillouin scattered light, containing Rayleigh and Brillouin peaks (Stokes and anti-Stokes), were fitted using the damped harmonic oscillator model where the exact position of these peaks determines the BFS. The BFS data was analysed using unsupervised clustering algorithm to identify similarity groups within the data and enable statistical analysis across cellular regions (cell centre, body, and periphery).

## Statistical Analysis

All experiments were conducted with a minimum of 3 biological replicates. Statistical significance was determined using Student's *t*-test, one-way, or two-way ANOVA (GraphPad Prism v. 8.2.1) with a Dunnett post-hoc analysis. Error bars represent SD or SEM (see figure legend for details). Significance was determined as  $p < 0.05$ .

## RESULTS

### Temperate Grass Pollen Species Show Diverse Physical Properties and Protein Expression

SEM images of dry, whole Ryegrass (Fig. 1A), and Timothy grass (Fig. 1B) showed distinct surface topography and displayed a rough, granular exine outer surface structure. Although dried, both grass pollen species were identified as being spheroidal and possessing a pore surrounded by an annulus (Fig. 1A–B, white arrows). Ryegrass and Timothy grass pollen proteins were extracted and subjected to gel electrophoresis. Coomassie staining of grass pollen protein extracts indicated varying protein compositions between the grass pollen species (Fig. 1C). Most notably was the abundance of known allergen proteins: group 1 allergen, Lol p 1 [21] at ~29 kDa and the group 5 allergen, Lol p 5 at ~29–31 kDa, present in the Ryegrass pollen extract (Fig. 1C; RG) when compared to Timothy grass pollen (Fig. 1C; TG). Both Lol p 1 and Lol p 5 are thought to be critical mediators of allergen mediated asthma attacks [22, 23] yet the minimal presence of either protein is an intriguing characteristic given the hypothesised role for Timothy grass pollens in inducing ETSA events.

### Exposure to Timothy Grass Pollen Rapidly Reduces Membrane Integrity and Induces Hypoxia

Pollen PPE first comes into contact with a cell at the lipid membrane, and therefore, we sought to determine if this initial contact altered membrane integrity. A549 respiratory epithelial cells were first pre-loaded with the Calcein-AM, a cell permeable compound that passively crosses the membrane, subsequently accumulating in the cytoplasm where it is cleaved by intracellular esterases to the fluorescent form. Thus, if the integrity of the membrane is decreased as a result of pollen exposure, Calcein will be released from the cell and intracellular fluorescence will be reduced [18]. A549 control cells showed stable fluorescence throughout the 30-min time course. However, those cells exposed to increasing concentrations of Timothy grass pollen proteins displayed a concentration-dependent decrease in fluorescence within the first 25–30 min (Fig. 1D), suggesting that Timothy grass pollen proteins had reduced the integrity of the membrane. Further to this, protein pollen extracts (PPE) have been shown to retain intrinsic NADPH oxidase activity that result in an increase in cellular ROS production [24] suggesting that exposure to

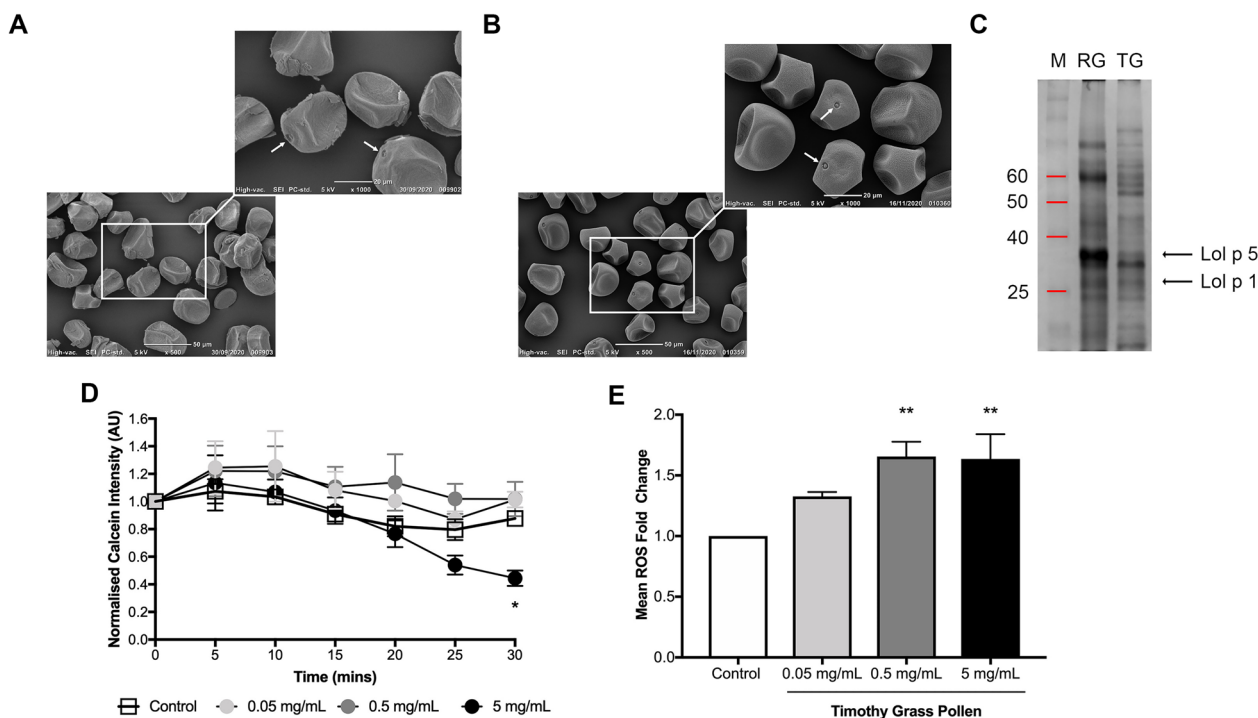


**Fig. 1** Scanning electron microscopy (SEM) images of dry, whole **A** Ryegrass and **B** Timothy grass pollens obtained at 5 kV. White arrows identify pores. Scale bar: 50  $\mu\text{m}$  and 20  $\mu\text{m}$  (inset). **C** Coomassie stain of Ryegrass (RG) and Timothy grass (TG) PPE. Molecular weight marker (M) shown in the first lane. **D** Fluorescence intensity of A549 cells treated with Calcein-AM and exposed to concentrations of Timothy grass PPE (0.05, 0.5, 0.5, or 5 mg/mL). Data expressed as normalised mean  $\pm$  SEM. Statistical analysis determined following Two-way ANOVA with Dunnett post-hoc analysis; \* $p < 0.05$ . **E** A549 cellular ROS production following exposure to Timothy grass PPE. Data expressed as normalised mean  $\pm$  SEM. Statistical analysis determined following one-way ANOVA with Dunnett post hoc analysis; \*\* $p < 0.01$ .

PPE may induce hypoxia in A549 cells. Expectedly, those cells exposed to either 0.5 or 5 mg/mL of PPE showed a significant increase in ROS production 24 h post exposure (Fig. 1E), together indicating that respiratory cell exposure to Timothy grass PPE exposure not only reduced membrane integrity but also induced hypoxia.

### Respiratory Cells Exposed to Timothy Grass PPE Triggered Spatial Reorganisation of Cytoskeletal Components

Cellular hypoxia has previously been shown to trigger activation of RhoA GTPase [11] and as such we next investigated known downstream process of activated RhoA GTPase, cytoskeletal organisation and abundance, and cell morphology. A549 control cells displayed characteristic dense F-actin bundles at cell borders known as the peri-junctional actin belt (Fig. 2; Control), while the

peri-junctional actin belt of cells exposed to increasing concentrations of Timothy grass PPE appeared less apparent, suggesting that exposure to pollen had altered the actin dynamics. Importantly, those cells treated with 5 mg/mL of Timothy grass PPE displayed ‘dash-like’, longitudinal actin fibres that traversed the cell body corresponding with a loss of the peri-junctional actin belt, suggesting that pollen-induced hypoxic conditions had indeed activated the RhoA GTPase pathway as proposed by Dada et al. (2007). To quantify this change in actin re-organisation, those cells treated with Timothy grass PPE were binned into 10 equidistant bins (Fig. 3A), with Bin 1 positioned at the centre of the cell and Bin 10 at the cell periphery (i.e., cell boundary) and the mean actin fluorescence intensity per bin determined. Cells treated with 5 mg/mL Timothy grass PPE showed a significantly higher mean F-actin fluorescence intensity in Bins 1–6 when compared to control (Fig. 3B), indicating an increase of F-actin present at the cell centre as observed in the cell images (Fig. 2).

Furthermore, the increase in central actin in these cells was accompanied by a significant decrease in mean actin fluorescent intensity at the cell boundary when compared to control cells (Fig. 3B; Bin 10), confirming the loss of peri-junctional actin observed in Fig. 2.

We next sought to determine if the spatial reorganisation of actin had influenced the organisation of additional cytoskeletal components and therefore investigated tubulin. Interestingly, we found that the increased presence of actin at the centre of the cell correlated with the loss of tubulin (Fig. 3C; Bins 1–6), suggesting that the two cytoskeletal networks work in synergy to maintain cell area (Fig. 3D) and shape (Fig. 3E). To determine if this spatial reorganisation of the cytoskeletal proteins was a result of increased protein expression, we performed western blot analysis of

cells exposed to Timothy grass PPE. Importantly, neither actin nor tubulin expression was altered following exposure to Timothy grass PPE (Fig. 3F, G), suggesting that the spatial reorganisation of the cytoskeletal proteins was not a result of altered protein levels.

### Cell Compressibility Is Decreased at the Cell Centre Following Exposure to Timothy Grass PPE

The pollen-induced change in membrane dynamics, coupled with the spatial reorganisation of actin, suggested that pollen may alter cellular viscoelasticity and compressibility. Brillouin microscopy was used to ascertain if

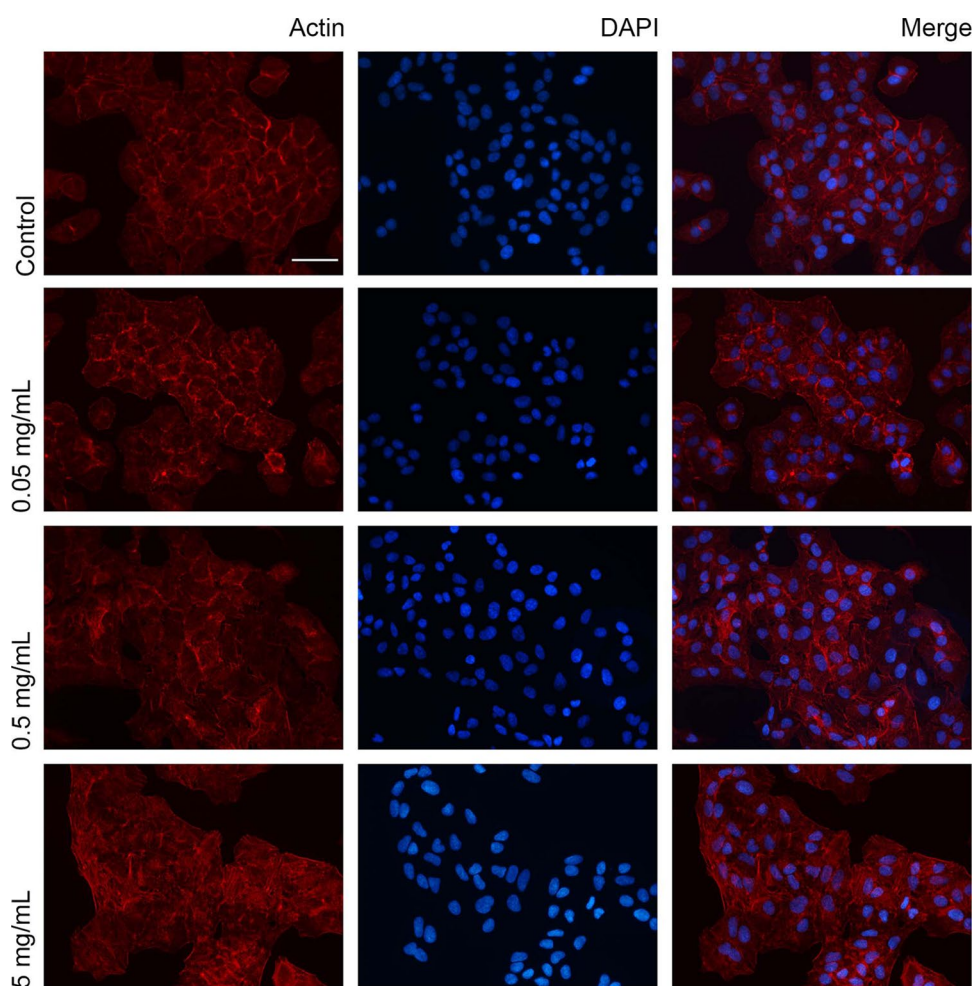


**Fig. 2** Representative images of A549 cells showing fluorescently labelled actin (red) and nucleus (blue). Merged images shown in the final panel. Cells were treated for 24 h with different concentrations of Timothy grass PPE (0.05, 0.5, 0.5, or 5 mg/mL). Scale bar: 50  $\mu$ m.

# Timothy Grass Pollen Induces Spatial Reorganisation of F-Actin and Loss of Junctional Integrity...

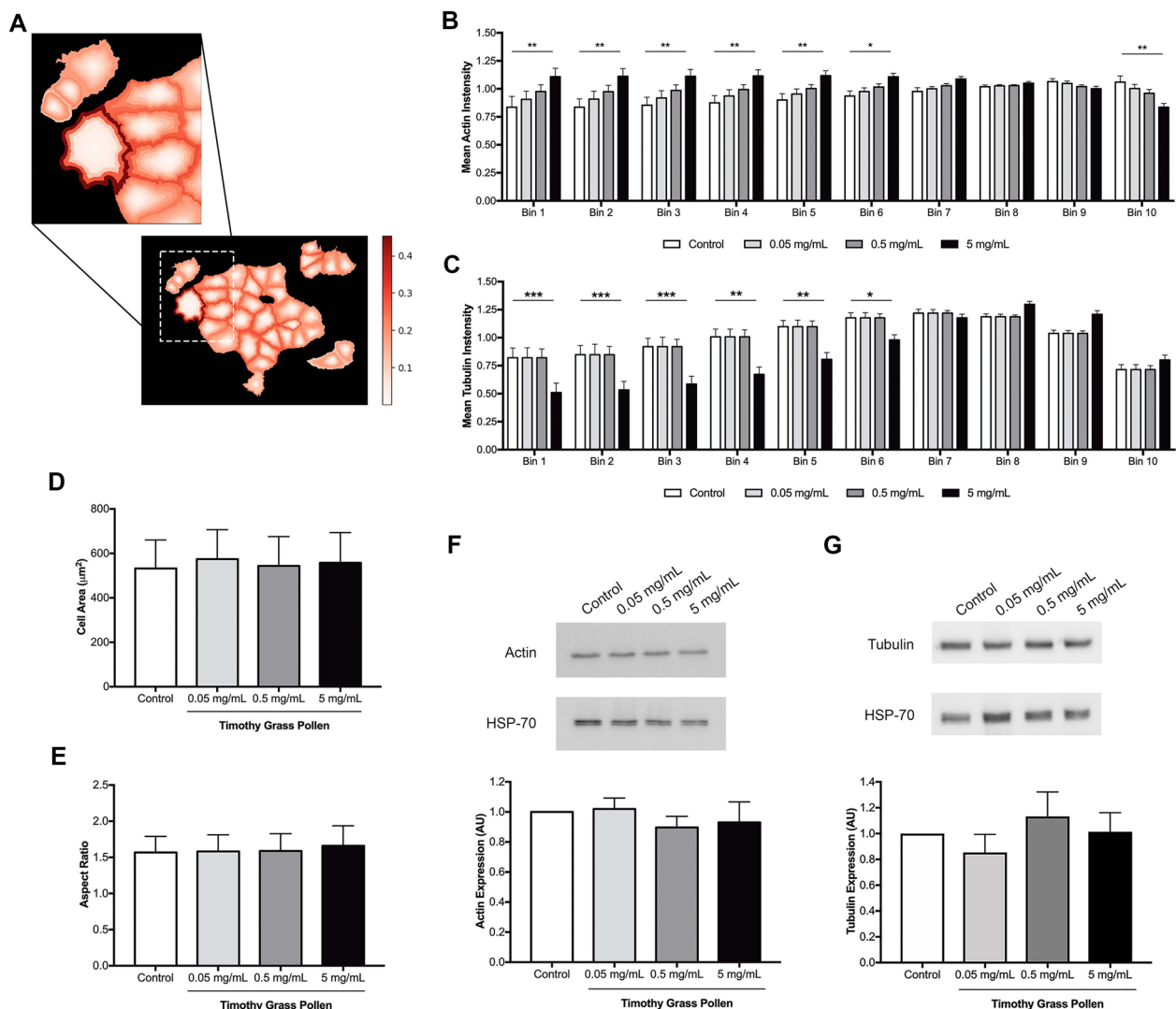
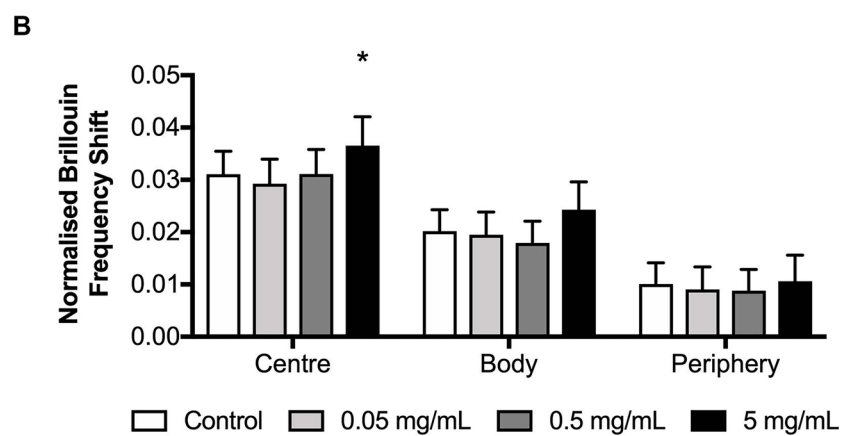
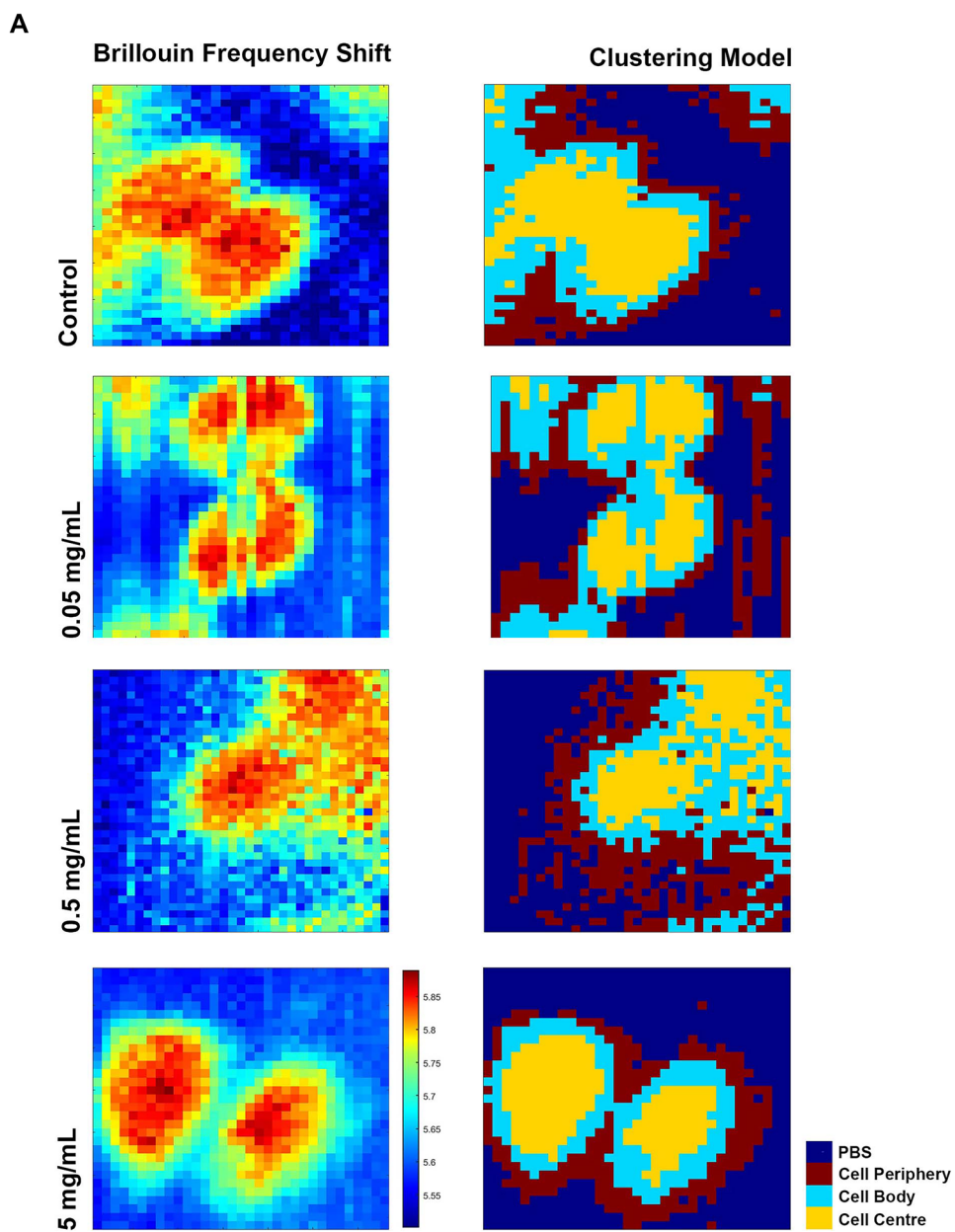


**Fig. 3** Actin fluorescence intensity was measured for cells following 24 h of Timothy grass PPE exposure. **A** Cells were binned into 10 equidistant, scaled bins to quantify the mean actin fluorescence intensity. **B** Mean integrated (sum) F-actin fluorescence intensity per cell was also measured following treatment with Timothy grass PPE. **C** Mean integrated (sum) tubulin fluorescence intensity per cell was also measured following treatment with Timothy grass PPE. A549 cell morphometry analysis following 24 h of grass PPE exposure **D** cell area and **E** aspect ratio. Total A549 protein expression (western blot and densitometry analysis; HSP-70 probed for loading control) of cytoskeletal components **F** Actin and **G** Tubulin. All data expressed as normalised mean ± SEM. Statistical analysis of **B** and **C** was determined following two-way ANOVA with Dunnett post hoc analysis, while **D**, **E**, **F**, **G** was determined following one-way ANOVA with Dunnett post hoc analysis; \**p* < 0.05, \*\**p* < 0.01.

pollen exposure altered the elasticity and compressibility of respiratory cells as the higher the Brillouin frequency shift (BFS), the stiffer and less compressible the cellular component (such as the nucleus) [25]. Alternatively, low BFS values are characteristic of softer cellular components with high hydration and elasticity (such as cell cytoplasm) [26]. To identify these cellular components,

an unsupervised clustering algorithm (K-means clustering) was used to segment the 2D maps of unlabelled cells into 4 separate groups, PBS, cell periphery, cell body, and cell centre (Fig. 4A). Thus, A549 cells exposed to 5 mg/mL Timothy grass PPE resulted in a significant increase in BFS at the cell centre (Fig. 4A, B), suggesting that the centre of the cell had become stiffer. Importantly, this



◀ **Fig. 4** **A** Representative 35  $\mu\text{m} \times 35 \mu\text{m}$  maps of Brillouin frequency shift (BFS) measured across the cells in  $XY$  plane (parallel to the surface of the tissue culture plastic). The colour scale represents the magnitude of the BFS that is attributed to the compressibility of the cell and surrounding PBS buffer. The unsupervised clustering algorithm ( $K$ -means clustering) and the effective recognition of features were used to segment the 2D maps of unlabelled cells into 4 separate groups, discriminating PBS (blue), the cell periphery (red), cell body (cyan), and the cell centre (yellow)-Colour Bar units GHz. **B** Normalised BFS. Data expressed as mean  $\pm$  SD. Statistical analysis determined following two-way ANOVA with Dunnett post hoc analysis; \* $p < 0.05$ .

increase in BFS correlated with the spatial reorganisation of actin observed previously (Fig. 3B) and therefore inferring that exposure to Timothy grass pollen had significantly reduced cell compressibility at the cell centre.

### Spatial Reorganisation of F-Actin Induces Inflammatory Response

Actin reorganisation is known to play an important role in regulating not only cell function but also the inflammatory response [27, 28]. Thus, given the known role inflammatory mediators play in exacerbating thunderstorm asthma, we hypothesised that the change in actin organisation observed in A549 cells following exposure to Timothy grass PPE would also induce an inflammatory response, specifically interleukin (IL)-6 and -8. Interestingly, exposing A549 cells to Timothy grass PPE did not induce detectable levels of IL-6 secretion at any of the concentrations tested (data not shown). However, A549 cells treated with increasing concentrations of Timothy grass PPE showed a significant increase in IL-8 secretion when treated with 5 mg/mL (Fig. 5A), correlating with the loss of actin from the peripheral belt. To determine if the increase in IL-8 secretion following exposure to 5 mg/mL Timothy grass PPE was in response to the spatial reorganisation of actin, we first stabilised actin filaments and then exposed the cells to 5 mg/mL Timothy grass PPE for 24 h (Fig. 5B, C). Importantly, no significant increase in IL-8 secretion was observed in those cells exposed to 5 mg/mL Timothy grass PPE when compared to control following stabilisation of the actin filaments (Fig. 5B). Taken together, these data highlight a molecular link between the spatial organisation of actin filaments and the inflammatory response.

### Timothy Grass PPE Reduced E-Cadherin Localisation to the Cell Boundary and Reduced Cell-Cell Junctional Barrier Integrity

The integrity of the cell membrane and the presence of F-actin organisation at the peri-junctional belt have both been identified as important determinants of cell-cell junction formation and integrity [29, 30]. Thus, we hypothesised that the pollen-induced changes to membrane integrity and F-actin may also alter cell-cell junctional integrity and therefore sought to determine the subcellular localisation of the known cell-cell junctional protein, E-cadherin. As the concentration of Timothy grass PPE increased, E-cadherin localisation to cell-cell junctions appeared to decrease, corresponding to the loss of the peri-junctional F-actin belt (Fig. 6). Fluorescence intensity measurements of E-cadherin at the cell boundary confirmed that cells treated with 5 mg/mL of Timothy grass PPE had significantly less E-cadherin localised to the cell boundary when compared to control (Fig. 7A). To ensure that this reduction in E-cadherin at the cell boundary was not due to a reduction in E-cadherin protein expression, we determined the fluorescence intensity of E-cadherin per cell and found no significant difference between any of the treatment groups (Fig. 7B). We further confirmed this by western blot, and expectedly, no significant difference in total E-cadherin expression was determined (Fig. 7C), suggesting the reduced E-cadherin localisation to cell boundaries was not a result of decreased E-cadherin protein levels.

Changes to E-cadherin subcellular localisation can alter cell-cell junctional barrier integrity, as such the barrier integrity of A549 monolayers exposed to temperate grass PPE was assessed over a 24 h period. Thus, changes in transepithelial electrical resistance (TEER) were measured in real time using ECIS [31]. A549 cells treated with 0.05 mg/mL Timothy grass PPE showed a significant increase in TEER (Fig. 7D), suggesting that at low concentrations, Timothy grass pollen may act to increase respiratory epithelial barrier quality. While those cells treated with 5 mg/mL Timothy grass PPE showed a significant decrease in TEER when compared to control (Fig. 7D), suggesting that the loss of the peri-actin belt and E-cadherin localisation to cell-cell junctions had reduced barrier integrity.

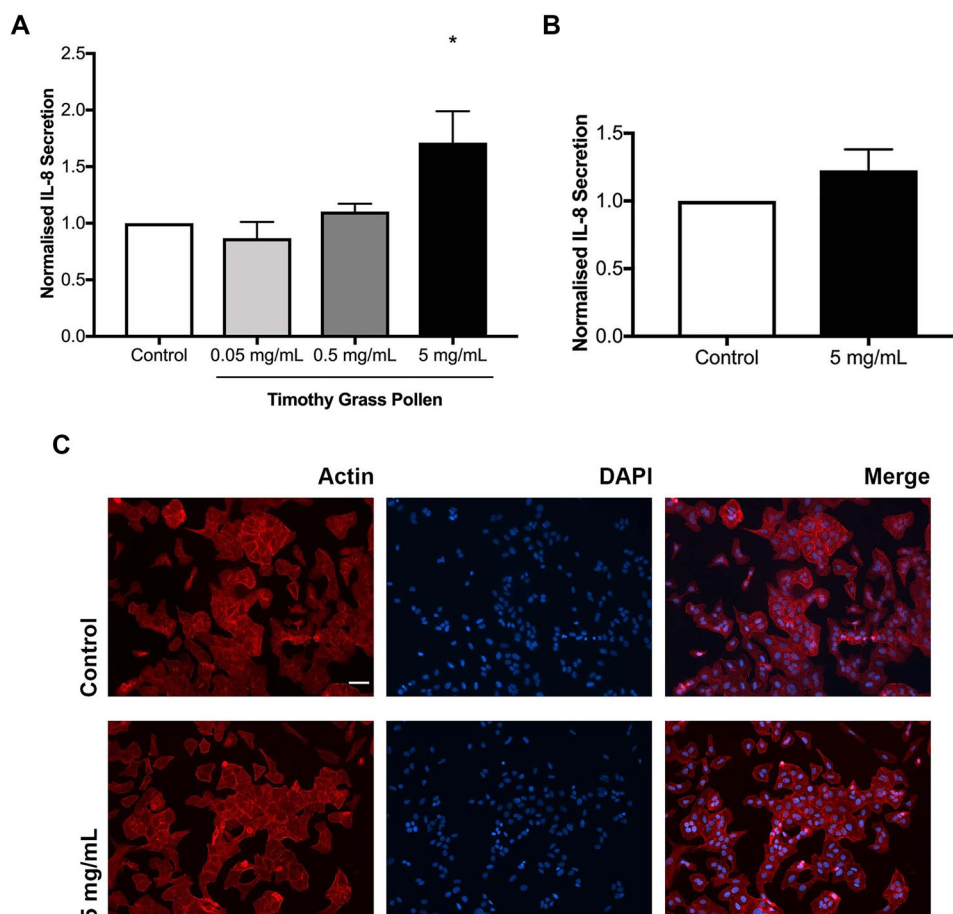


**Fig. 5** **A** IL-8 cytokine release 24 h post treatment with Timothy grass PPE. Data expressed as normalised mean  $\pm$  SEM. Statistical analysis determined following one-way ANOVA with Dunnett post hoc analysis; \* $p < 0.05$ . **B** IL-8 cytokine release of cells pre-treated with phalloidin and then exposed to Timothy grass PPE. Data expressed as normalised mean  $\pm$  SEM. Statistical analysis determined following Student's *t*-test; \* $p < 0.05$ . **C** Representative images of A549 cells showing fluorescently labelled actin (red) and nucleus (blue). Merged images shown in the final panel. Cells were pre-treated with phalloidin to stabilise actin filaments and then exposed to Timothy grass PPE.

## DISCUSSION

Temperate grass pollen species are known to have varying compositions of allergen group proteins [21, 32], and it is the inhalation of these allergens that penetrate the lower airways, causing the severe asthma attacks often associated with pollen exposure [22, 23, 33]. It has been hypothesised that the Lol p 5 allergen proteins of pollen granules may be responsible for triggering an epidemic of thunderstorm asthma [22, 34] and yet Timothy grass PPE showed a minimal amount of Lol p 5 allergen protein. Intriguingly however, despite the lack of Lol p 5, Timothy grass PPE triggered significant actin and tubulin

reorganisation in respiratory epithelial cells, ultimately altering respiratory cell behaviour and function.

Pollen proteins first encounter the respiratory cell surface at the plasma membrane and here we show that within minutes of exposure to pollen proteins, the integrity of the A549 cell membrane is altered. Further to this, PPEs are known to retain NADPH activity that can induce oxidative stress in A549 cells [24]; our data suggests that PPE-mediated hypoxia is concentration dependant, with only high concentrations of Timothy grass PPE significantly increasing ROS production after 24 h. Interestingly, oxidative stress has been shown to reduce Na, K<sup>+</sup> ATPase activity [35], a transmembrane osmotic

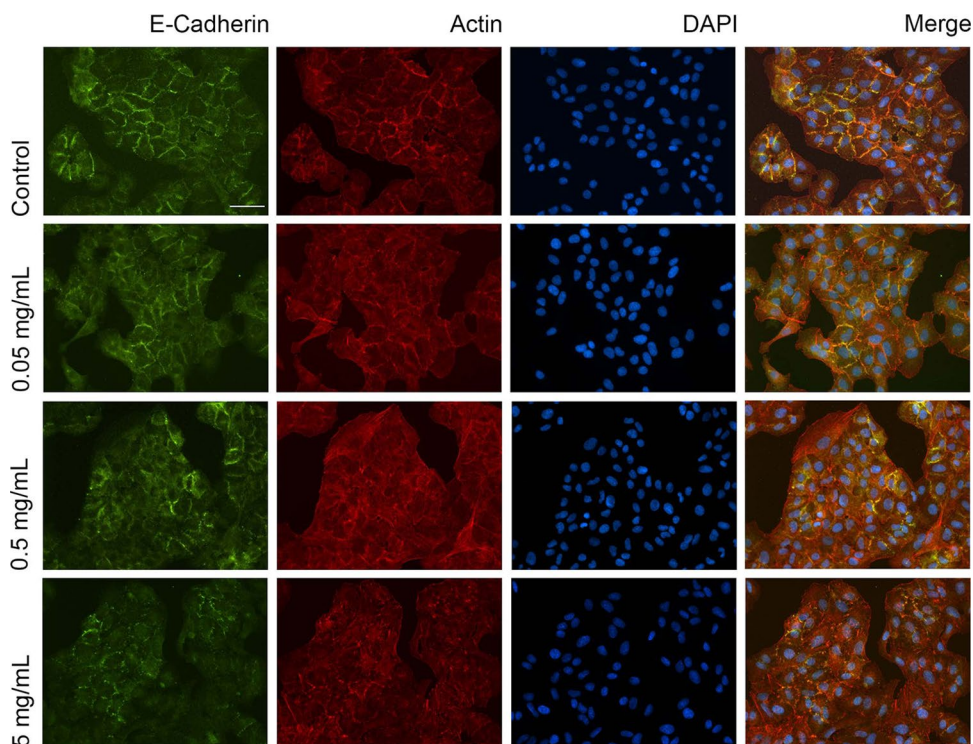


**Fig. 6** Representative images of A549 cells immunostained with E-cadherin (green) and fluorescently co-labelled actin (red) and nucleus (blue). Merged images shown in the final panel. Cells were treated for 24 h with different concentrations (0.05, 0.5, 0.5, or 5 mg/mL) Timothy grass PPE. Scale bar: 50  $\mu$ m.

regulator protein that functions to maintain transepithelial osmotic gradient and therefore epithelial barrier integrity; thus, we hypothesise that pollen destabilises membrane integrity and increases ROS activity to then downregulate Na, K + ATPase activity.

Pollen-induced spatial reorganisation of F-actin triggered the release of F-actin from the peri-junctional belt, causing actin filaments to form stress fibres that traverse the cell body (Figs. 2 and 3B). Importantly, this pollen-induced change in actin organisation coincided with an equal and opposite change in microtubule organisation (Fig. 3C). As F-actin was redistributed from the peri-junctional ring to a more centralised stress fibre configuration, the density of microtubule network at the cell centre was reduced to accommodate the spatial reorganisation of F-actin. This finding is in agreement with several other studies that have shown actin regulates the microtubule organisation of epithelial cells [36, 37]. Importantly, this re-organisation of the cytoskeletal components did not change cell size or shape, but it did reduce compressibility of the respiratory cells (Fig. 4) possibly

increasing cell stiffness [38] that may contribute to the acute bronchospasms observed during ETSA events. Further to this, our data agrees with previous studies that has highlighted a role for actin dynamics in regulating the inflammatory response (reviewed in [39]), as the reorganisation of actin filaments was shown to induce secretion of the proinflammatory cytokine, IL-8 (Fig. 5).

Cell-cell junctions play an essential role in maintaining not only barrier integrity but also determine proliferation, cell mechanical integrity, and barrier function [40]. Our findings suggest that while total E-cadherin expression remained unchanged (Fig. 7C), subcellular localisation of E-cadherin to cell-cell junctions had been disrupted following exposure to Timothy grass pollen extract (Fig. 6). Importantly, decreased E-cadherin staining has previously been found in oral swabs of people suffering from severe allergies [41], suggesting that loss of E-cadherin at the cell boundary may be an important indicator of Timothy grass mediated effects on the respiratory cell epithelium. Structurally, E-cadherin plays an important role in regulating the cell-cell junctional

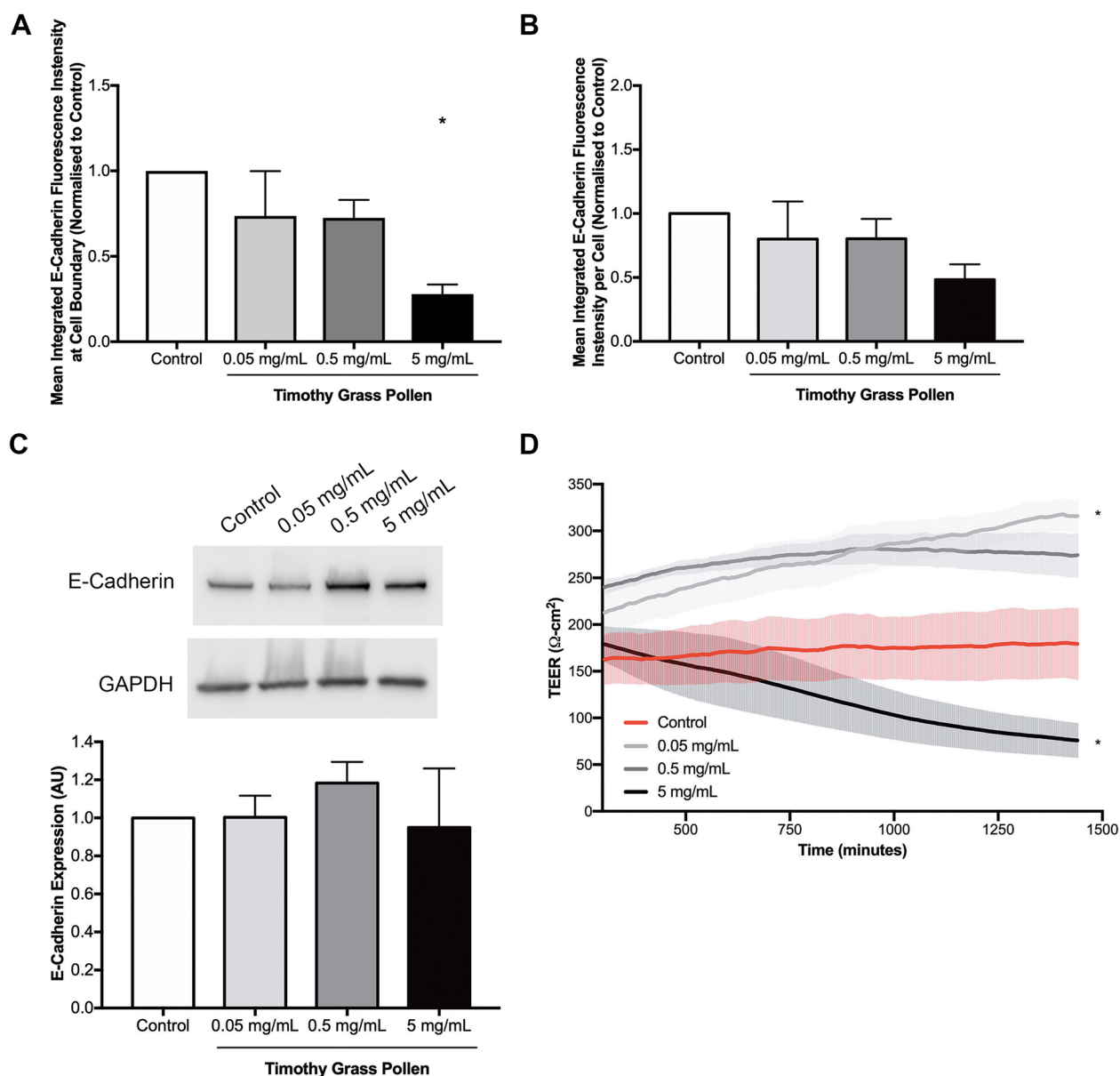


**Fig. 7** Quantification of E-cadherin fluorescence intensity **A** at the cell boundary and **B** per cell following 24 h treatment of Timothy grass PPE. **C** E-cadherin protein expression (western blot and densitometry analysis; GAPDH probed for loading control) following exposure to Timothy grass PPE. **D** Real-time TEER quantification of cells treated with Timothy grass PPE. Data expressed as mean  $\pm$  SEM. Statistical analysis determined following one-way ANOVA with Dunnett post hoc analysis; \* $p < 0.05$ .

integrity. Our findings suggest that at low concentrations, Timothy grass PPE increased respiratory epithelial barrier quality, yet surprisingly, we observed no increase in E-cadherin fluorescence at the cell boundary. In contrast, cells exposed to high concentrations of Timothy grass PPE were shown to display a significant decrease

in respiratory barrier integrity, correlating with the loss of both F-actin and E-cadherin from the cell boundary.

It has been previously shown that modifications to the lipid composition of cell membranes [30] as well as increased ROS production (i.e., reduced Na, K + ATPase activity) [42, 43] trigger the loss of E-cadherin from

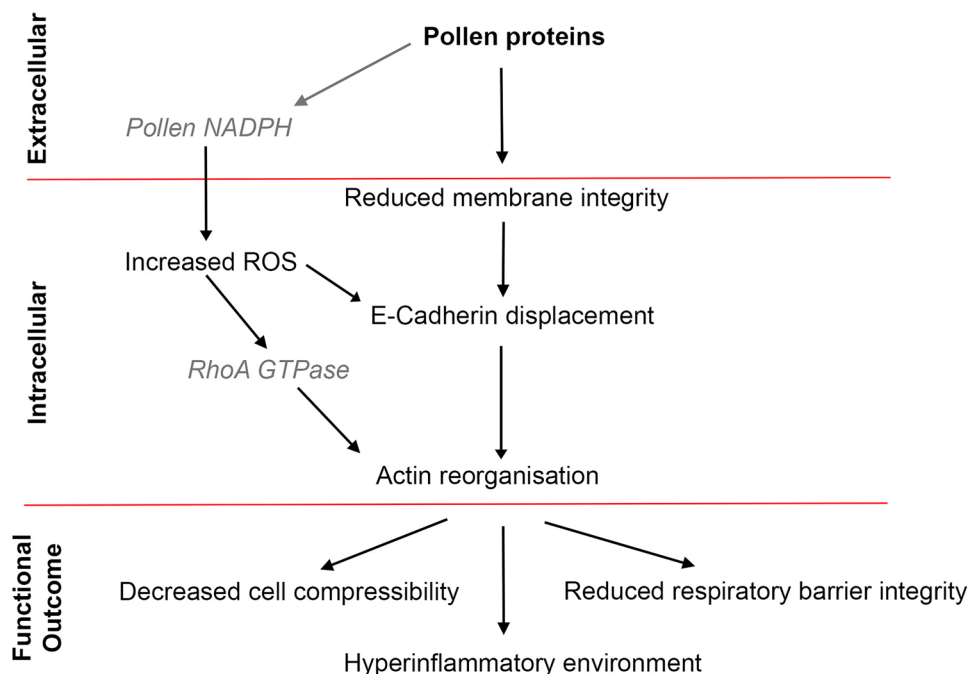


**Fig. 8** The hypothesised molecular pathway that contributes to ETSA severity. Pollen proteins work in concert to disrupt the integrity of the lipid membrane and increase intracellular ROS to displace E-cadherin from cell–cell-junctions. This in turn triggers the spatial reorganisation of the actin cytoskeleton that together result in reduced cell compressibility, reduced barrier integrity and the hallmark of ETSA events, a hyperinflammatory environment.

cell–cell junctions resulting in spatial reorganisation of cytoskeletal components [44]. Thus, we propose that pollen proteins may first act in concert to destabilise the integrity of the phospholipid membrane and increase ROS production, prompting the release of E-cadherin from the cell–cell junctions and triggering the spatial reorganisation of both actin and tubulin cytoskeletal components (Fig. 8). Functionally, this proposed pathway culminates in the reduction of respiratory luminal barrier integrity and hyperinflammatory environment consistent with the acute respiratory distress observed during ETSA.

## ACKNOWLEDGEMENTS

The authors would like to thank Maree Svolos (Respiratory Technology, Woolcock Institute of Medical Research, Glebe, Australia) for her helpful discussions.

## AUTHOR CONTRIBUTION

PB and AC contributed equally towards concept development, data curation, manuscript preparation, and figure preparation. HM

and IK conducted Brillouin microscopy data curation and analysis. HO, DT, JMD, IK, PS, and SP provided critical feedback.

## FUNDING

Funding issued by Australian Research Council; ARC DP190100376, ARC DP190101973. Australian Research Council, DP190100376

## AVAILABILITY OF DATA AND MATERIALS

Not applicable.

## DECLARATIONS

**Ethics Approval and Consent to Participate** Not applicable.

**Consent for Publication** All authors consent for publication.

**Competing Interests** The authors declare no competing interests.

## REFERENCES

- Dabrera, G., V. Murray, J. Emberlin, J.G. Ayres, C. Collier, Y. Clewlow, et al. 2013. Thunderstorm asthma: An overview of the evidence base and implications for public health advice. *QJM* 106 (3): 207–217.
- Thien, F., J.M. Davies, M. Hew, J.A. Douglass, and R.E. O’Hehir. 2020. Thunderstorm asthma: An overview of mechanisms and management strategies. *Expert Review of Clinical Immunology* 16 (10): 1005–1017.
- Campbell, S.L., P.D. Fox-Hughes, P.J. Jones, T.A. Remenyi, K. Chappell, C.J. White, et al. 2019. Evaluating the risk of epidemic thunderstorm asthma: Lessons from Australia. *International Journal of Environmental Research and Public Health*. 16 (5): 837.
- Bannister, T., D. Csutoros, A.L. Arnold, J. Black, G. Feren, R. Russell, et al. 2020. Are convergence lines associated with high asthma presentation days? A case-control study in Melbourne, Australia. *Science Total Environment* 737 : 140263.
- Andrew, E., Z. Nehme, S. Bernard, M.J. Abramson, E. Newbigin, B. Piper, et al. 2017. Stormy weather: a retrospective analysis of demand for emergency medical services during epidemic thunderstorm asthma. *Bmj* 359 : j5636.
- Thien, F., P.J. Beggs, D. Csutoros, J. Darvall, M. Hew, J.M. Davies, et al. 2018. The Melbourne epidemic thunderstorm asthma event 2016: An investigation of environmental triggers, effect on health services, and patient risk factors. *Lancet Planet Health*. 2 (6): e255–e263.
- dos Remedios, C.G., D. Chhabra, M. Kekic, I.V. Dedova, M. Tsubakihara, D.A. Berry, et al. 2003. Actin binding proteins: Regulation of cytoskeletal microfilaments. *Physiological Reviews* 83 (2): 433–473.
- Ingber, D.E. 2008. Tensegrity and mechanotransduction. *Journal of Bodywork and Movement Therapies* 12 (3): 198–200.
- Chalut, K.J., and E.K. Paluch. 2016. The actin cortex: A bridge between cell shape and function. *Developmental Cell* 38 (6): 571–573.
- Fletcher, D.A., and R.D. Mullins. 2010. Cell mechanics and the cytoskeleton. *Nature* 463 (7280): 485–492.
- Dada, L.A., E. Novoa, E. Lecuona, H. Sun, and J.I. Sznajder. 2007. Role of the small GTPase RhoA in the hypoxia-induced decrease of plasma membrane Na, K-ATPase in A549 cells. *Journal of Cell Science* 120 (Pt 13): 2214–2222.
- Gloushankova, N.A., S.N. Rubtsova, I.Y. Zhitnyak. 2017. Cadherin-mediated cell-cell interactions in normal and cancer cells. *Tissue Barriers* 5 (3): e1356900.
- Smyrek, I., B. Mathew, S.C. Fischer, S.M. Lissek, S. Becker, E.H.K. Stelzer. 2019. E-cadherin, actin, microtubules and FAK dominate different spheroid formation phases and important elements of tissue integrity. *Biology Open* 8 (1).
- Mège, R.M., N. Ishiyama. 2017. Integration of cadherin adhesion and cytoskeleton at adherens junctions. *Cold Spring Harbor Perspectives in Biology* 9 (5).
- Baum, B., and M. Georgiou. 2011. Dynamics of adherens junctions in epithelial establishment, maintenance, and remodeling. *Journal of Cell Biology* 192 (6): 907–917.
- Aghapour, M., P. Racc, S.J. Moghaddam, P.S. Hiemstra, and I.H. Heijink. 2018. Airway epithelial barrier dysfunction in chronic obstructive pulmonary disease: Role of cigarette smoke exposure. *American Journal of Respiratory Cell and Molecular Biology* 58 (2): 157–169.
- Davies, J.M., M.L. Bright, J.M. Rolland, and R.E. O’Hehir. 2005. Bahia grass pollen specific IgE is common in seasonal rhinitis patients but has limited cross-reactivity with Ryegrass. *Allergy* 60 (2): 251–255.
- Molina-Guijarro, J.M., A. Macias, C. Garcia, E. Munoz, L.F. Garcia-Fernandez, M. David, et al. 2011. Irvalec inserts into the plasma membrane causing rapid loss of integrity and necrotic cell death in tumor cells. *PLoS One* 6 (4): e19042.
- Lee, E., E.A. Shelden, and D.A. Knecht. 1998. Formation of F-actin aggregates in cells treated with actin stabilizing drugs. *Cell Motility and the Cytoskeleton* 39 (2): 122–133.
- McQuin, C., A. Goodman, V. Chernyshev, L. Kamensky, B.A. Cimini, K.W. Karhohs, et al. 2018. CellProfiler 3.0: Next-generation image processing for biology. *PLoS Biology* 16 (7): e2005970.
- Davies, J.M., D. Mittag, T.D. Dang, K. Symons, A. Voskamp, J.M. Rolland, et al. 2008. Molecular cloning, expression and immunological characterisation of Pas n 1, the major allergen of Bahia grass *Paspalum notatum* pollen. *Molecular Immunology* 46 (2): 286–293.
- Hew, M., J. Lee, N. Varese, P.M. Aui, C.I. McKenzie, B.D. Wines, et al. 2020. Epidemic thunderstorm asthma susceptibility from sensitization to ryegrass (*Lolium perenne*) pollen and major allergen Lol p 5. *Allergy* 75 (9): 2369–2372.
- Suphioglu, C., M.B. Singh, P. Taylor, R. Bellomo, P. Holmes, R. Puy, et al. 1992. Mechanism of grass-pollen-induced asthma. *Lancet* 339 (8793): 569–572.
- Boldogh, I., A. Bacsı, B.K. Choudhury, N. Dharajiya, R. Alam, T.K. Hazra, et al. 2005. ROS generated by pollen NADPH oxidase provide a signal that augments antigen-induced allergic airway inflammation. *The Journal of Clinical Investigation* 115 (8): 2169–2179.
- Scarcelli, G., W.J. Polacheck, H.T. Nia, K. Patel, A.J. Grodzinsky, R.D. Kamm, et al. 2015. Noncontact three-dimensional mapping of intracellular hydromechanical properties by Brillouin microscopy. *Nature Methods* 12 (12): 1132–1134.
- Wu, P.J., I.V. Kabakova, J.W. Ruberti, J.M. Sherwood, I.E. Dunlop, C. Paterson, et al. 2018. Water content, not stiffness, dominates Brillouin spectroscopy measurements in hydrated materials. *Nature Methods* 15 (8): 561–562.
- Liu, X. 2008. Inflammatory cytokines augments TGF-beta1-induced epithelial-mesenchymal transition in A549 cells by up-regulating TbetaR-I. *Cell Motility and the Cytoskeleton* 65 (12): 935–944.
- Du, L., J. Zhou, J. Zhang, M. Yan, L. Gong, X. Liu, et al. 2012. Actin filament reorganization is a key step in lung inflammation induced by systemic inflammatory response syndrome. *American Journal of Respiratory Cell and Molecular Biology* 47 (5): 597–603.
- Madara, J.L., R. Moore, and S. Carlson. 1987. Alteration of intestinal tight junction structure and permeability by cytoskeletal contraction. *American Journal of Physiology* 253 (6 Pt 1): C854–C861.
- Marquez, M.G., N.O. Favale, F. Leocata Nieto, L.G. Pescio, and N. Sterin-Speziale. 2012. Changes in membrane lipid composition cause alterations in epithelial cell-cell adhesion structures in renal papillary collecting duct cells. *Biochimica et Biophysica Acta* 1818 (3): 491–501.
- Szulcek, R., H.J. Bogaard, G.P. van Nieuw Amerongen. 2014. Electric cell-substrate impedance sensing for the quantification of endothelial proliferation, barrier function, and motility. *Journal of Visualized Experiments* (85).
- Fenaille, F., E. Nony, H. Chabre, A. Lautrette, M.N. Couret, T. Batard, et al. 2009. Mass spectrometric investigation of molecular variability of grass pollen group 1 allergens. *Journal of Proteome Research* 8 (8): 4014–4027.

## Timothy Grass Pollen Induces Spatial Reorganisation of F-Actin and Loss of Junctional Integrity...

33. Bacsi, A., B.K. Choudhury, N. Dharajiya, S. Sur, and I. Boldogh. 2006. Subpollen particles: Carriers of allergenic proteins and oxidases. *The Journal of Allergy and Clinical Immunology* 118 (4): 844–850.
34. Knox, R.B. 1993. Grass pollen, thunderstorms and asthma. *Clinical and Experimental Allergy* 23 (5): 354–359.
35. Dada, L.A., N.S. Chandel, K.M. Ridge, C. Pedemonte, A.M. Bertorello, and J.I. Sznajder. 2003. Hypoxia-induced endocytosis of Na, K-ATPase in alveolar epithelial cells is mediated by mitochondrial reactive oxygen species and PKC-zeta. *The Journal of Clinical Investigation* 111 (7): 1057–1064.
36. Dugina, V., I. Alieva, N. Khromova, I. Kireev, P.W. Gunning, P. Kopnin. 2016. Interaction of microtubules with the actin cytoskeleton via cross-talk of EB1-containing +TIPs and  $\gamma$ -actin in epithelial cells. *Oncotarget* 7 (45).
37. Alberico, E.O., Z.C. Zhu, Y.O. Wu, M.K. Gardner, D.R. Kovar, and H.V. Goodson. 2016. Interactions between the microtubule binding protein EB1 and F-actin. *Journal of Molecular Biology* 428 (6): 1304–1314.
38. Smith, P.G., L. Deng, J.J. Fredberg, and G.N. Maksym. 2003. Mechanical strain increases cell stiffness through cytoskeletal filament reorganization. *American Journal of Physiology. Lung Cellular and Molecular Physiology* 285 (2): L456–L463.
39. Ivanov, A.I., C.A. Parkos, and A. Nusrat. 2010. Cytoskeletal regulation of epithelial barrier function during inflammation. *American Journal of Pathology* 177 (2): 512–524.
40. Garcia, M.A., W.J. Nelson, N. Chavez. 2018. Cell-cell junctions organize structural and signaling networks. *Cold Spring Harb Perspect Biology* 10 (4).
41. Rosace, D., C. Gomez-Casado, P. Fernandez, M. Perez-Gordo, M.D.C. Dominguez, A. Vega, et al. 2019. Profilin-mediated food-induced allergic reactions are associated with oral epithelial remodeling. *The Journal of Allergy and Clinical Immunology* 143 (2): 681–90.e1.
42. Mandel LJ., R.B. Doctor, R. Bacallao. 1994. ATP depletion: a novel method to study junctional properties in epithelial tissues: II. Internalization of Na<sup>+</sup>,K<sup>+</sup>-ATPase and E-cadherin. *Journal of Cell Science* 107 : 3315–3324.
43. Rajasekaran, S.A., L.G. Palmer, K. Quan, J.F. Harper, W.J. BJ, H.H. Bander, A.P. Soler, A.K. Rajasekaran. 2001. Na,K-ATPase beta-subunit is required for epithelial polarization, suppression of invasion, and cell motility. *Molecular biology of the cell* 12 : 279–295.
44. Zhitnyak, IY, S.N. Rubtsova, N.I. Litovka, N.A. 2020. Gloushankova. Early events in actin cytoskeleton dynamics and E-cadherin-mediated cell-cell adhesion during epithelial-mesenchymal transition. *Cells* 9 (3).

**Publisher's Note** Springer Nature remains neutral with regard to jurisdictional claims in published maps and institutional affiliations.